Transactions on the Built Environment vol 66, © 2003 WIT Press, www.witpress.com, ISSN 1743-3509

Modelling micro-structure aspects of masonry walls by a simplified approach

S. Casolo & F. Peña
Dipartimento di Ingegneria Strutturale, Politecnico di Milana, Italy

Abstract

A specific simplified rigid element approach is proposed to model the elastic-plastic behaviour of masonry walls subjected to in-plane loadings. This proposal originates from the consideration that the evaluation of seismic vulnerability of masonry monuments requires peculiar procedures since their responses to earthquakes often differ substantially from those of ordinary buildings. In particular, the effective characterisation of the masonry material requires a special attention because the global mechanical behaviour of this composite material depends strongly on the different textures, as well as on the elastic-plastic characteristics of the component materials. Numerical analyses are made with the objective of evaluating the importance of the micro-structure effects in the response of masonry walls with special attention to the fact that mechanical degradation tends to concentrate in the weaker component according to a well defined pattern. The paper is limited to the case of monotonic loadings as a first step in the formulation of a rigid element model that is suitable for performing complete dynamical analyses.

1 Introduction

Earthquake damage surveys show that seismic response of historical buildings often differs substantially from those of ordinary buildings. As a consequence, in this case vulnerability analysis requires specific approaches. The present numerical model is proposed with the belief that the formulation of an effective simplified model in this field should be based on two considerations: i) the main phenomenon that should be modelled in order to study the global performance of a building subjected to earthquakes is the

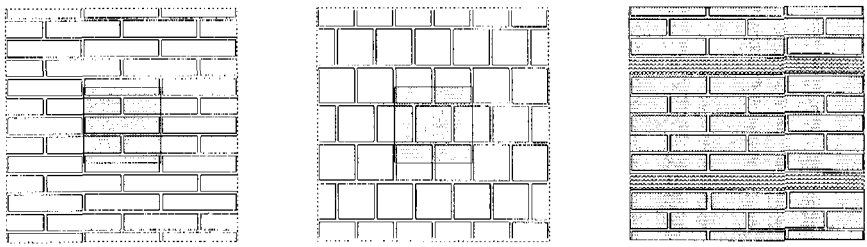

Figure 1: Examples of the different running bond textures studied.

transmission and transformation of seismic energy from the ground into the structure [1]; ii) the seismic loading is very complex, thus a reliable estimation of seismic risk to such buildings requires studies in which a number of different forcing actions selected on the basis of appropriate considerations about seismic intensity are applied to the numerical models [2, 3]. The consequence of these general lines is to give preference to discrete models that are suitable for studying the seismic response of entire portions of a building - e.g. the façade and lateral walls of a church, the bell tower [4] - by performing complete dynamical analyses. In this context, a numerical model should be designed as to allow the description of the global hysteretic behaviour, at least by means of a simplified fenomenological approach [5, 6, 7].

In the present paper only monotonic in-plane loadings will be considered as a first step toward the formulation of a rigid model suitable for an easy subsequent improvement to perform complete dynamical analyses including the hysteretic behaviour. Some attention have been devoted to the microstructure characteristics, and the three regular textures shown in Figure 1 have been considered in particular. The geometry of traditional Italian bricks has been adopted for the rectangular units: $l \times d \times h = 25 \times 12 \times 5.5$ cm^3. The dimensions of the square bricks are: $l \times d \times h = 12 \times 12 \times 12$ cm^3. The height of the timber layers is $h = 5.5$ cm. The thickness of the mortar joints is $t = 1$ cm. The vertical head-joints, interrupted by the bricks, are generally of poor quality and weaker than the horizontal continuous bed-joints. As a first approach, the case of single leaf masonry is considered here for simplicity. The proposed rigid elements are quadrilateral, and each adjoining couple is connected by three elastic-plastic devices that can be thought as linear springs. These connections are defined with attention to the texture characteristics that should be ascribed to the simplified discrete model at the macro-scale. This approach has the advantage to allow a simplified description of the elastic-plastic response by simply defining the elemental behaviour of the axial and shear connections that are considered as separate springs.

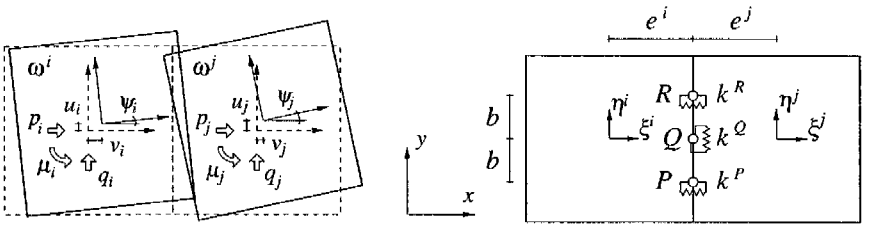

Figure 2: Couple of rigid elements. Notation and disposition of the springs.

2 Model discretization

The plain domain Ω is partitioned into m quadrilateral elements ω^i such that no vertex of one quadrilateral lies on the edge of another quadrilateral. A local reference frame $\{o^i, \xi^i, \eta^i\}$ is placed in each element barycentre o^i, with the ξ^i-axis initially parallel to the global x-axis as shown in the example of Figure 2. The deformed configuration of the discrete model is described by the variations of position of these local reference frames that move remaining fixed to the elements. Three kinematic variables, the two translations u_i, v_i and the rotation angle ψ_i, are associated to each element, and the whole kinematic configuration is described by the $3m$ Lagrangian coordinates assembled in the vector $\{u\}$:

$$\{u\}^T = \{u_1, v_1, \psi_1, u_2, v_2, \psi_2, \ldots, u_m, v_m, \psi_m\} \ . \tag{1}$$

The external loads, including the inertial forces, are applied considering the undeformed geometry. For each element ω^i, they are condensed in three resultants: the horizontal and the vertical forces p_i and q_i, applied in the barycentre o^i, and the couple μ_i. The m triplets $\{p_i, q_i, \mu_i\}$ are assembled into a vector of generalised external loads $\{p\}$, conjugate with vector $\{u\}$, as follows:

$$\{p\}^T = \{p_1, q_1, \mu_1, p_2, q_2, \mu_2, \ldots, p_m, q_m, \mu_m\} \ . \tag{2}$$

The elastic devices that connect each couple of elements are placed in correspondence of three connection points named P, Q and R, as shown in Figure 2, right. A *shear elastic connection* is placed in the mid-point Q, while two *normal elastic connections* are placed in the external points P and R, at a distance b from Q. The elastic force in each device depends on a measure of mean strain associated to the corresponding connection point: a shear strain ε^Q is associated with point Q, while axial strains ε^P and ε^R, are associated with points P and R. The vector of generalised strains $\{\varepsilon\}$ is assembled in order to contain all the measures of mean strain as follows:

$$\{\varepsilon\}^T = \left\{\varepsilon_1^P, \varepsilon_1^Q, \varepsilon_1^R, \varepsilon_2^P, \varepsilon_2^Q, \varepsilon_2^R, \ldots, \varepsilon_s^P, \varepsilon_s^Q, \varepsilon_s^R\right\} \ . \tag{3}$$

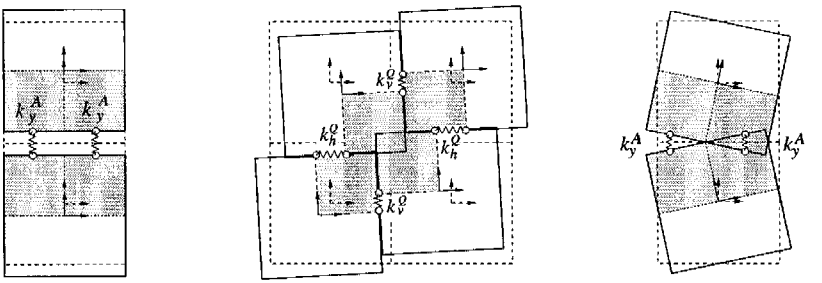

Figure 3: Axial, shear and in-plane bending deformations.

being s the number of sides that connect the elements of the whole discrete model. Then, in the small displacement field, the linearity allows to express the strain-displacement relations by considering a $s \times m$ matrix $[B]$:

$$\{\varepsilon\} = [B]\{u\} \ . \tag{4}$$

3 Elastic-plastic identification

3.1 Elastic behaviour

The identification of the elastic parameters of the discrete model is performed by means of a computational approach in which we consider the response of a sub-domain of the periodic composite material that include all the component materials and that constitute the entire structure by periodicity [8]. For simplicity, in this presentation we make reference to the square periodic cells shown in Figure 1 with shaded areas. The rigid elements adopted for the identification are also squares aligned with the principal axes of the material. The size of these elements is the same of the periodic cells, i.e. $2e$. The elastic characteristics of the connecting devices are assigned with the criterion of approximating the strain energy of the corresponding volumes of pertinence in the cases of simple deformation. Two axial, one symmetric shear, and two in-plane flexural loadings are considered for the direct numerical identification. The composite material has been analysed by means of a generalised plane strain finite element model adopting the proper loading and periodic boundary conditions [9].

The axial behaviour is characterised by equal actions in the two normal connecting devices of the common side as shown in Figure 3, left, where the area of the volume of pertinence corresponding to the two normal elastic connection is shaded. Two tests, one for horizontal and one for vertical axial stiffness are needed. Given the mean measures of strain $\varepsilon_x = u/e$ and $\varepsilon_y = v/e$, and the corresponding average elastic energy densities $\mathcal{U}_x^A$ and $\mathcal{U}_y^A$, then the two generalised axial stiffnesses per unit volume to be

attributed to the normal connecting devices, k_x^A and k_y^A, are calculated as follows:

$$k_x^A = \frac{2\,\mathcal{U}_x^A}{\varepsilon_x^2} \quad , \quad k_y^A = \frac{2\,\mathcal{U}_y^A}{\varepsilon_y^2} \; . \tag{5}$$

It is clear that these normal connections cannot account for the Poisson coupling effect.

The symmetric shear behaviour is characterised by equal forces in the shear connecting devices of the four sides of each square element. Figure 3, centre, shows this case with reference to an assemblage of four rigid elements; the shaded area corresponds to half of the volume of pertinence of the four shear connecting devices. The finite element analyses reveal that in this case the deformation of the bricks is a mix of shear and bending, plus a "local" rigid rotation of the bricks that can be considered as a sort of characteristic *micro-rotation* [10]. If the global rigid rotation of the finite domain is prevented, then the average symmetric shear strain is $\varepsilon_s = u/e = v/e$, while the micro-rotation can be reproduced by means of the rotation degree of freedom of the rigid elements. In particular, if we adopt square rigid elements whose size equals the periodic cell, then the local rigid rotation of the bricks for the "rectangular" and "square" running bond textures can be simply assigned as the rotation ψ of the rigid elements. In fact in these textures the "local" rigid rotation is identical for all the bricks of the periodic cell. On the other side, the "wooden" running bond the "local" rigid rotation depends on the position of the single brick respect to the timber layers, thus it is better to consider an average value of rotation. In any case, Casolo [10] proposed as a "local" measure of the generalised shear strains for the vertical and the horizontal connecting devices of the rigid elements the following expressions:

$$\begin{aligned} \varepsilon_v &= \varepsilon_s - \psi = \varepsilon_s\,(1-\rho) \\ \varepsilon_h &= \varepsilon_s + \psi = \varepsilon_s\,(1+\rho) \end{aligned} \tag{6}$$

being $\rho = \psi/\varepsilon_s$. The equilibrium of the shear stresses implies that the stiffnesses of the shear connecting devices of the vertical and of the horizontal sides are related by the following equation:

$$\frac{k_h^Q}{k_v^Q} = \frac{\varepsilon_v}{\varepsilon_h} = \frac{1-\rho}{1+\rho} \; . \tag{7}$$

Thus, we can write:

$$k_h^Q = k_s(1-\rho) \quad , \quad k_v^Q = k_s(1+\rho) \; . \tag{8}$$

being k_s the generalised symmetric shear stiffness defined as follows

$$k_s = \frac{\mathcal{U}_s}{(1-\rho^2)\varepsilon_s^2} \; . \tag{9}$$

Table 1: Elastic moduli of the components [MPa].

material	E_x	E_y	G
brick	5000	5000	2273
horizontal mortar	1667	1667	758
vertical mortar	555	555	252
wood	10000	300	500

Table 2: Elastic characteristics for rigid elements [MPa],[-].

texture	k_x	k_y	k_s	ρ
rectangular	3844	3722	1572	-0.076
square	3171	4095	1497	-0.101
wooden	4620	1411	1182	0.187

The distance b of the normal connections from the mid-point of each side must be defined in order to model the in-plane flexural rigidity between the elements. In the present formulation, the case of linear stress distribution along a common side of length $2e$ is simulated by placing the normal connecting devices in the Gauss points, i.e. $b = e/\sqrt{3}$. In general, the value of b can be assigned in order to approximate other types of stress distributions.

With reference to the three textures shown in Figure 1, just as an example, we assigned the values reported in Table 1 to the elastic characteristics of the finite element models. The bricks and the mortar are assumed as isotropic with $\nu = 0.1$, while the wood is orthotropic. The results of the corresponding identification are reported in Table 2.

3.2 Plastic behaviour

The plastic behaviour of the composite textures has been analysed by means of a computational approach. The wood is defined as simply elastic, while a Drucker-Prager material model has been assigned to the bricks and to the mortar joints. In particular, the shape of the yield surface in the meridional plane is hyperbolic in order to assign a tension cut-off [11]. The values that define the plastic behaviour are reported in Table 3. Angle β is the friction angle at high confining pressure, while p_t is the hydrostatic tension strength. Isotropic softening is defined for bricks, with evolution of the yield surface defined by giving the uniaxial compression yield stress σ_c, while a slight isotropic hardening is defined for the mortar joints. The softening and hardening behaviours are defined by a second value of stress σ_y together with the corresponding plastic strain ϵ_y [11]. Perfect bond between materials is assumed. The response of the finite element models

Table 3: Angles [degrees] and tractions [MPa] assigned to the Drucker-Prager material model for monotonic finite element analyses.

material	β	p_t	σ_c	σ_y	ϵ_y
brick	20^o	1.00	25.	3.0	0.005
horizontal mortar	25^o	0.10	3.0	3.1	0.001
vertical mortar	25^o	0.04	1.0	1.1	0.001

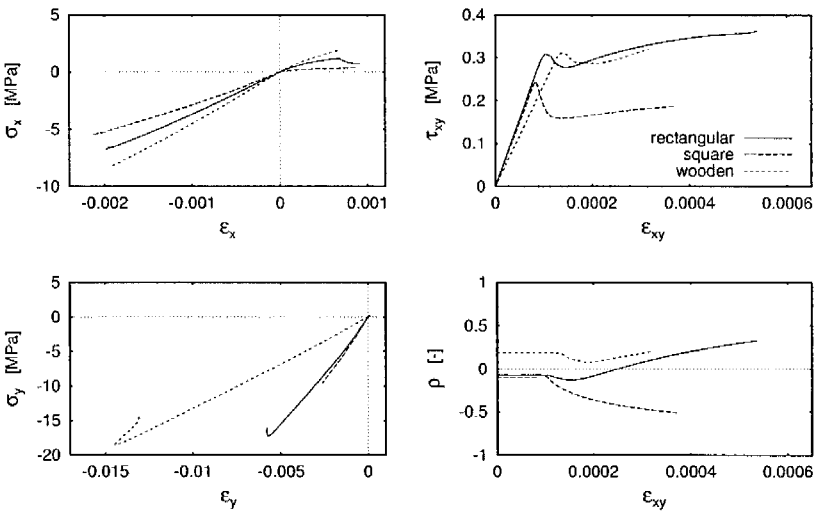

Figure 4: Monotonic responses of the finite element models of the three textures subjected to horizontal and vertical axial loading (σ_x and σ_y), and to symmetric shear loading (τ_{xy}).

of the periodic cells of the three textures is shown in Figure 4. It is worth comparing the responses of the different textures. In particular we note that the insertion of the timber layers tends to soften all the three responses of the composite without compromising the strength, while the square brick texture appears as the weakest for all the aspects. The graph that reports the trend of the micro-rotation ratio ρ as a function of the mean symmetric shear strain shows that the micro-rotation effect varies and increases in a different manner for the different textures as a function of the mechanical degradation. Keeping in mind that the present numerical approach should be considered just as a first example in order to test the proposed model, these responses constitute the base for defining the elastic-plastic monotonic behaviour to be attributed to the connections of the rigid elements, and the

Table 4: Tensile strengths f_{tx} and f_{ty}, cohesion c [MPa], and friction angle β [degrees] for the connection devices of the rigid element model.

texture	f_{tx}	f_{ty}	c	β
rectangular	0.750	0.230	0.294	25^o
square	0.300	0.234	0.240	25^o
wooden	1.850	0.230	0.290	25^o

stress-strain curves of Figure 4 have been fitted by piece-wise linear relations that have been assigned to the connecting springs. At this stage, symmetric stiffness and strength have been attributed to the shear connections, thus we do not consider the loss of shear symmetry due to the micro-rotation effect. The main parameters that define the plastic behaviour of the connection devices of the rigid element model are reported in Table 4. The tensile strength of the axial connections along x and y are respectively f_{tx} and f_{ty}. The plastic response of each axial connection is independent from the behaviour of any other connection, while the shear strength is related to the stresses of the axial connections of the same side according with Mohr-Coulomb criterion [12].

4 Numerical application

As a first application of the proposed model, the simple masonry piers shown in Figure 5 have been calculated and compared using three detailed finite element models and a simple rigid element model with only $3 \times 6 = 18$ elements. The finite element models consider the effective texture of the composite materials, and the meshes for rectangular, square and wooden running bond textures have 2880, 2592 and 2880 elements, respectively. A constant vertical pressure q equal to 0.5 MPa was applied at the top,

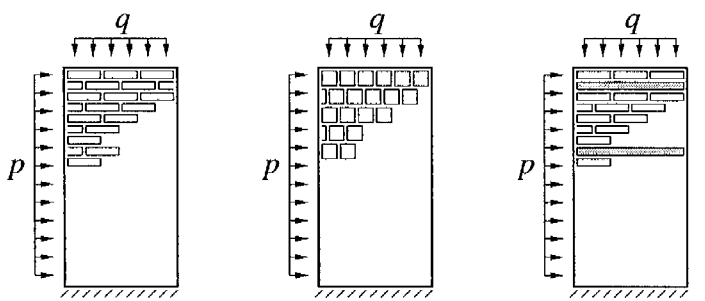

Figure 5: Examples of walls with different running bond textures.

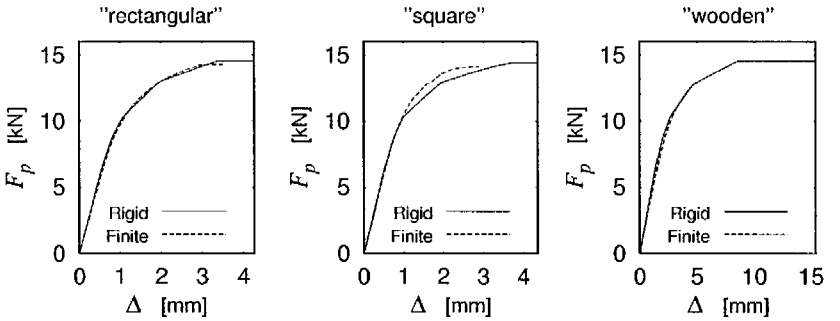

Figure 6: Lateral force - lateral displacement relations.

while the lateral loading p progressively increased. The comparison of the responses in terms of total lateral force F_p and lateral displacement at the top Δ is shown in Figure 6. The differences of strength between the three textures are small because in this case the collapse mechanism is essentially flexural, and we have the stabilizing effect of the vertical load. The "square" texture is only slightly weaker than the others two, while the benefit of the "wooden" texture can be appreciated essentially in terms of greater ductility. In any case, the differences between rigid elements' and finite elements' responses are small.

5 Final remarks

The present approach is the first step toward the formulation of a model for studying the in-plane seismic response of masonry walls made with regular textures using very few degrees of freedom. Adopting rigid elements, the procedure of identification has been developed with the aim of considering some of the micro-structure characteristics that can be significant for high ratios between the elastic moduli of the bricks and the mortar. This is often the case of masonry walls subjected to loadings related with strong seismic events, when mortar response is out-of the linear elastic field. Since the present study is propaeudetic in view of the subsequent implementation of the hysteretic response and mechanical degradation of the material, a main feature of this approach is to allow the separate formulation for the axial and the shear hysteretic behaviour that are simply related by Mohr-Coulomb criterion.

Acknowledgement

The second author was supported by a grant of the Mexican National Council for Science and Technology (CONACYT).

References

[1] Bertero, V.V., Innovative approaches to earthquake engineering (Chapter 1). *Innovative Approaches to Earthquake Engineering*, ed. G. Oliveto, WIT press, pp. 1-54, 2002.

[2] Petrini, V., Overview report on vulnerability assessment. *Proc. 5th Int. Conf. on Seismic Zonation,* Nice, **III** pp. 1977-1988, 1995.

[3] Petrini, V. & Casolo, S., Vulnerability of historical and monumental buildings: significant ground motion parameters and evaluation of the seismic performance (Chapter 4). *Innovative Approaches to Earthquake Engineering*, ed. G. Oliveto, WIT press, pp. 203-228, 2002.

[4] Petrini, V., Casolo, S. & Doglioni, F., Models for vulnerability analysis of monuments and strengthening criteria. *Proc. XI European Conf. on Earthquake Engineering, Paris*, Invited lecture volume, pp. 179-198, Balkema: Rotterdam, 1999.

[5] Casolo, S., A Three-dimensional model for vulnerability analysis of slender medieval masonry towers. *Journal of Earthquake Engineering*, **2**(4), pp. 487-512, 1998.

[6] Casolo S., & Boffi G., Un modello ad elementi rigidi per gli archi in muratura, *XIV Congresso Nazionale AIMETA*, CD-ROM, Como, Italy, 6-9 ottobre 1999.

[7] Casolo, S., Modelling the out-of-plane seismic behaviour of masonry walls by rigid elements. *Earthquake Engineering and Structural Dynamics*, **29**(12), pp. 1797-1813, 2000.

[8] Michel J.C., Moulinec H., & Suquet P., Effective properties of composite materials with periodic microstructure: a computational approach. *Computer Methods in Applied Mechanics and Engineering* **172**, pp. 109-143, 1999.

[9] Anthoine A., Homogenization of periodic masonry: plane stress, generalized plane strain or 3D modelling? *Communications in Numerical Methods in Engineering*, **13**, pp. 319-326, 1997.

[10] Casolo S., In plane dynamics of masonry walls by rigid elements: elastic behaviour and micro-structure effects. *GIMC 2002, Third Joint Conference of Italian Group of Computational Mechanics*, CD-ROM, Giulianova, Italy, 24-26 June 2002.

[11] ABAQUS Version 5.6, *Theory and Users' manuals*, Hibbit, Karlsson & Sorensen, Inc. U.S.A. 1996.

[12] Peña F., Rigid element model for dynamic analysis of in-plane masonry structures. *Ph. D. thesis*, Politecnico di Milano, December 2001.